

# Enhancing concrete performance at high temperatures through polypropylene fiber geometry optimization

Bhawani Antarvedi<sup>a,b</sup>, Nawal Kishor Banjara<sup>a,b\*</sup> & Suvir Singh<sup>a,b</sup>

<sup>a</sup>CSIR- Central Building Research Institute, Roorkee 247 667, India

<sup>b</sup>Academy of Scientific and Innovative Research, Ghaziabad 201 002, India

Received: 07 May 2024; accepted: 10 November 2024

This article has explored the optimization of polypropylene fiber dosage and geometry to enhance the thermal stability of high-performance concrete under fire exposure. In this study, experimental investigations have been carried out on plain concrete and polypropylene fibre-reinforced concrete (PFRC) at higher temperatures. The study has been performed at different temperatures, including ambient temperature and temperatures ranging from 200 °C to 1000 °C. Visual inspection, mass loss, mechanical properties, non-destructive testing, and microstructural analyses have been conducted on plain concrete and PFRC specimens. It has been found that the impact of polypropylene fibres in concrete has become more significant when exposed to higher temperatures. The findings indicate that selecting an optimum length and dosage of fibers has been necessary to prevent concrete spalling. Additionally, the diameter of PP fibers has been found to have no notable impact on preventing spalling. This research has also examined the effectiveness of adding Macro fiber polypropylene of length 24mm to the concrete. The effect of adding PP fibres in concrete has been analyzed while assessing mass loss, compressive strength, tensile and flexural strength, and UPV values at higher temperatures.

**Keywords:** Elevated temperature, Non-destructive testing, Plain concrete, Polypropylene fibres

## 1 Introduction

One of the most dangerous environmental conditions to which structures are exposed is fire, Kodur et al., (2014)<sup>1</sup>. Because concrete is a heterogeneous material, each constituent behaves differently at high temperatures. Further more, the physical properties of the concrete change with an increase in temperature. As a result, Handoo et al., (2002)<sup>2</sup> reported that when exposed to fire, concrete's mechanical properties, such as strength, Young's modulus, volume stability, etc., may change and it may behave violently due to the occurrence of concrete spalling. Concrete spalling is defined as a sudden loss of concrete cover that can be violent or non-violent in nature Khoury et al., (2000)<sup>3</sup>. Usually, two theories are accepted by scientific community on the origins of spalling: Pore pressure development and induced thermal stress. Despite advancements in studying spalling mechanisms, accumulating significant experimental data, and developing numerical models, predicting the behavior of concrete in fire remains highly challenging. This challenge stems from the multitude of influencing parameters

such as material composition, testing conditions, storage conditions, and more. Kalifa et al., (2001)<sup>4</sup>; A. Bilodeau et al., (2004)<sup>5</sup>; C.C. Han et al., (2005)<sup>6</sup>; P. Shuttleworth et al., (2001)<sup>7</sup>; Y.S. Heo et al., (2012)<sup>8</sup> found out that one of the most effective preventive measures against concrete spalling caused by fire involves adding polypropylene fibers (PP fibers) at a rate of a few kg/m<sup>3</sup> into the fresh concrete mixture. Before delving into the mechanisms through which PP fibers enhance the fire resistance of concrete and prevent spalling, basic information about polypropylene material is provided.

Polypropylene is a thermoplastic semi-crystalline polyolefin material, comprising 55% crystalline and 45% amorphous phases at room temperature Khoury et al., (2008)<sup>9</sup>. It finds utility in various applications due to its outstanding physical, mechanical, and thermal properties.

A pivotal characteristic of any thermoplastic material is its melting temperature. Melting involves the destruction of the crystalline phase and a subsequent decrease in mechanical properties associated with crystallinity. W. H. Bednarek et al., (2021)<sup>10</sup> mentioned in his paper that the melting temperatures are determined by the crystallinity phases:  $\alpha$ -phase crystallinity melts around 160-170 °C,

\*Corresponding author  
(E-mail: nawalkishor@cbri.res.in, nawal1234@gmail.com)

while  $\beta$ -phase melts around 150 °C. The material's melting occurs across a temperature range; however, for practical purposes, the peak value of the differential scanning calorimetry curve is considered the melting temperature. According to Khoury *et al.*, (2008)<sup>9</sup>, polypropylene's melting initiates at 150 °C, peaks at 165 °C, and concludes around 176 °C.

It is widely accepted that polypropylene (PP) fibers, upon melting, infiltrate into the pores and cracks of the cementitious material as is mentioned in paper by Y. Li *et al.*, (2018)<sup>11</sup>, where they are partially absorbed by the cementitious matrix by A. Noumowé *et al.*, (2005)<sup>12</sup>. This process creates empty channels that facilitate the improved evacuation of water vapor. These vacated channels contribute to an increase in the intrinsic permeability of concrete at high temperatures as is reported in papers by P. Kalifa *et al.*, (2001)<sup>4</sup>, A. Bilodeau *et al.*, (2004)<sup>5</sup>, I. Hager *et al.*, (2019)<sup>13</sup>, a reduction in pore pressure P. Kalifa *et al.*, (2001)<sup>4</sup>, and a decrease in spalling propensity P. Kalifa *et al.*, (2001)<sup>4</sup>; A. Bilodeau *et al.*, (2004)<sup>5</sup>; C.C. Han *et al.*, (2005)<sup>6</sup>; P. Shuttleworth *et al.*, (2001)<sup>14</sup>. G.A Khoury *et al.*, (2008)<sup>9</sup> mentioned in his paper that the additional characteristics of PP fibers in concrete that enhance spalling resistance include: i) the generation of air bubbles during mixing due to the presence of fibers, ii) the presence of an interface transitional zone (ITZ) around fibers with higher porosity compared to the matrix S. Askarinejad *et al.*, (2017)<sup>15</sup>, iii) the absence of adhesion between the fiber and matrix, which can allow steam passage as is mentioned by G.A Khoury *et al.*, (2008)<sup>9</sup>, and iv) microcracking around fibers due to the differential thermal expansion of fibers and matrix by D. Zhang *et al.*, (2018)<sup>16</sup>.

Fibers play a crucial role in enhancing the percolation of water vapor transport channels, which is essential for effective water vapor evacuation in heated concrete. Achieving percolation of fibers between each other is challenging with the conventionally proposed dosage of 2 kg/m<sup>3</sup>, or 0.22% volume E.J. Garboczi *et al.*, (1995)<sup>17</sup>; D.P Bentz *et al.*, (2000)<sup>18</sup>, suggesting the need to explore alternative percolation possibilities. He also suggests enhancing percolation by bridging the interface transition zone (ITZ) of aggregates with polypropylene (PP) fibers. G. Mazzucco *et al.*, (2015)<sup>19</sup> proposed other methods to improve connectivity include linking the ITZ of aggregates with the ITZ of fibers and pores and connecting thermally induced cracks at the paste-aggregate interface with PP fibers.

Several studies have been conducted to explore the impact of dosage and dimensions (length and diameter) of polypropylene (PP) fibers on the high-temperature behavior of concrete, aiming to identify the most effective solution for utilizing PP fibers. Various authors such as Kalifa *et al.*, (2001)<sup>4</sup>; Y. Li *et al.*, (2018)<sup>11</sup>; I. Hager *et al.*, (2019)<sup>13</sup>; Suhaendi S.L. *et al.*, (2006)<sup>20</sup>; Haniche R. *et al.*, (2001)<sup>21</sup>; F. Lu *et al.*, (2011)<sup>22</sup> have observed that higher PP fiber dosages lead to increased permeability, greater pore pressure drop during heating [Kalifa *et al.*, (2001)<sup>4</sup>; F. Lu *et al.*, (2011)<sup>22</sup>, and reduced spalling by Y.S.Heo., (2012)<sup>23</sup>; Y.S.Heo., (2011)<sup>24</sup>; Y. Li *et al.*, (2019)<sup>25</sup>; R. Jansson *et al.*, (2008)<sup>26</sup>. Concerning fiber length, longer fibers are generally more effective than shorter ones, as they tend to increase permeability, Y. Li *et al.*, (2019)<sup>25</sup>, gas pore pressure drop, S.L. Suhaendi *et al.*, (2006)<sup>20</sup>, and improve spalling resistance as mentioned by A. Bilodeau *et al.*, (2004)<sup>5</sup>; Y.S.Heo., (2011)<sup>24</sup>. Studies comparing PP fibers of different diameters at equal dosages reveal that thinner fibers result in the highest increase in permeability F. Lu *et al.*, (2016)<sup>22</sup> and lesser spalling by I. Knack., (2009)<sup>27</sup> due to their higher quantity. However, for an equal total number of fibers, there seems to be no significant impact of fiber diameter on spalling prevention, as is said by Y S Heo *et al.*, (2012)<sup>23</sup>. Despite the extensive experimental data providing insights into how PP fibers affect spalling tendency, the optimal choice of fibers to prevent spalling remains an unanswered question.

Improving the percolation of water vapor transport channels, thereby preventing concrete spalling during fire incidents, can be achieved through the optimization of polypropylene (PP) fiber selection. One effective approach to enhance this percolation is by connecting thermally induced cracks, resulting from differential thermal expansions between the matrix and aggregates, with PP fibers.

In the present study, we aim at optimizing the PP fibers of length 24mm to prevent spalling of concrete due to fire exposure with reduced dosage, the reason being explained above. It involves the utilization of polypropylene fibres of low modulus, in concrete to prevent the development of thermal cracks followed by spalling, when concrete is subjected to elevated temperatures up to 1000 °C. The positive effects of polypropylene fibre are brought about by the micro-cracking of cement paste [Huismann *et al.*, (2012)<sup>28</sup>, Pistol *et al.*, (2014)<sup>29</sup> and Felicetti *et al.*, (2017)<sup>30</sup>,

which results in thermal and moisture gradients, the development of lower water pressure in the concrete pores, and which may possibly give relaxation in thermal stress. First, tests in muffle furnace imitating standard ISO fire curve on concrete specimens containing various PP fiber geometries and dosages are performed. Based on these results, optimal fiber dosage is provided and discussed.

**1.1 Research significance**

The study presented fire test results demonstrating the impact of dosage, length, and diameter of polypropylene (PP) fibers on the spalling tendency of cementitious materials under elevated temperatures. These experimental findings are crucial for optimizing the selection of fibers needed to prevent concrete spalling.

This research will examine the effectiveness of adding Macro fiber polypropylene of length 24mm in the concrete to reduce the risk of concrete spalling. The experimental studies conducted in this paper aimed to optimize the selection of PP fiber geometry with the goal of preventing spalling in concrete exposed to fire. The use of polypropylene fibres in concrete to reduce fire spalling of concrete is a common practice when building tunnels and when using high strength concrete for ordinary buildings. According to Eurocode, (EN-1992)<sup>31</sup>, the dosage is recommended to be 2kg/m<sup>3</sup> with microfilament fibers. However, in the present study, the macro fibers is used with diameter and length much larger than the usual fibers used for reducing the spalling, for which most of the literature is available. Therefore, the dosage is also reduced than the recommended value in the Eurocode(EN -1992)<sup>31</sup>.

The effect of adding Macro polypropylene fibers in slabs, when it is subjected to elevated temperature is studied.

**2 Materials and Methods**

An experimental investigation is carried out to understand the influence of polypropylene fibre-reinforced concrete which is exposed to elevated temperatures. Polypropylene fibre is chosen as it increases the toughness of the concrete and helps in preventing spalling of the concrete when exposed to elevated temperature by Khoury*et al.*,(2008)<sup>9</sup>. In this study, concrete is exposed to various temperatures ranging from 200°C to 1000 °C and residual mechanical properties of the concrete are evaluated.

**2.1 Materials used in this study**

Ordinary Portland Cement (OPC) of 43 grade conforming to IS: 8112, (1989)<sup>32</sup> was used in this experimental work. According to IS: 4031, (1999)<sup>33</sup> parts IV, V, and VI, the consistency of cement, initial setting time, final setting time, and compressive strength of cement were assessed. The results are shown in Table 1. All of the test results are found to be within the recommended standards.

Fine aggregate properties were evaluated using the procedures outlined in IS: 2386, (1963)<sup>34</sup>. Fine aggregate properties such as specific gravity, water absorption, and gradation are important properties to consider when determining the suitability of aggregates and are also required for concrete mix proportioning. In the study, the fine aggregate was made from locally available river sand. The fine aggregate was a dark grey colour. The aggregates were dried in the sun before being sieved with a 4.75 mm sieve to remove the coarser material. Specific gravity was found to be 2.64 and water absorption was found to be 1.3%. IS: 2386 (Part I)<sup>34</sup> (1963) was used to determine the particle size distribution of fine aggregate. Similarly, the coarse aggregate properties which are used in this study were determined.

**2.2 Polypropylene fibers**

**2.2.1 Physical properties**

The polypropylene fibers that are used in this experimental study was fibrillated and white in colour as shown in Fig. 1. Polypropylene fibers are low modulus fiber with advantageous properties when used in concrete like good bonding adhesion, enhanced mechanical properties, long-term durability and better post – cracking behaviour to concrete. These fibers are non-corrosive, chemically inert and alkali resistant. An image of the fibre diameter from a

Table 1 — Properties of cement tested as per IS 4031: (1999)<sup>33</sup>.

Parameter	Test value	IS 8112: 1989 Recommendation
Standard consistency (% of water by wt. of cement)	29	-
Setting time (Minutes)		
a) Initial	60	30 (Min.)
b) Final	300	600 (Max.)
Compressive strength (MPa)		
After 3 days	27.5	23 (Min.)
1) After 7 days	39.2	33 (Min.)
2) After 28 days	46.8	43 (Min.)
Soundness (mm)	1.4	10(Max)
Fineness		
By air permeability (m <sup>2</sup> /kg)	355	225 (Min.)

filament was taken during the SEM study of the polypropylene fibres. The image acquired is displayed in Fig. 2. The properties of PP fibres used in this study (length-24mm) are given in Table 2.



Fig. 1 — Polypropylene fibres.

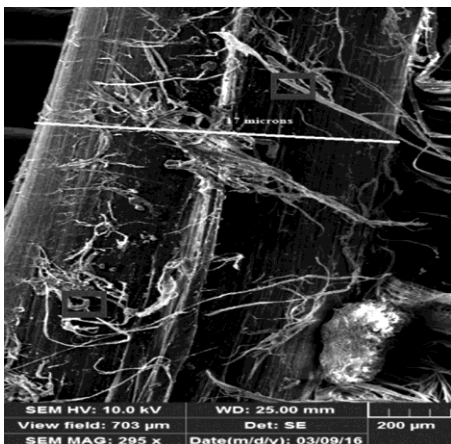


Fig. 2 — SEM image of polypropylene fibres.

### 2.2.2 Chemical composition

The chemical constitution of this PP fibres was also investigated. The EDAX analysis is then performed using the acquired SEM image. The distinctive peaks of the elemental analysis of PP fibre are shown in Fig. 3. According to the obtained EDAX curve, PP fibre appears to have a larger oxygen concentration but a minimal Si content.

### 2.2.3 X-Ray diffraction of PP fibres

Fibers made of polypropylene were given an XRD pattern. PP fibres were found to be crystalline in nature. Organic substances like dimethyl phenyl are present. Because of how it was made, there are organic molecules present (synthetic fiber). The XRD pattern for PP fibres is displayed in Fig. 4. Although the compounds that may be present in PP fibres can be determined by the relative counts of electrons emitted in SEM, XRD was used to achieve the true compound analysis.

### 2.2.4 TGA and DTA analysis

For PP fibres, thermal analysis using TGA and DTA was carried out. Few peaks were visible in the

Table 2 — Physical properties of polypropylene fiber.

Properties	Values	Remarks
Form	Monofilament	fibrillated
Length (mm)	24.0	Measured
Diameter ( $\mu\text{m}$ )	17	Measured
Aspect Ratio (L/D)	159	Calculated
Specific Gravity	0.90	Measured
Tensile strength (MPa)	678	Measured
Elastic modulus (GPa)	0.68	Data given in
Failure Strain (%)	19.1	Technical sheet
Melting Point ( $^{\circ}\text{C}$ )	168	Measured

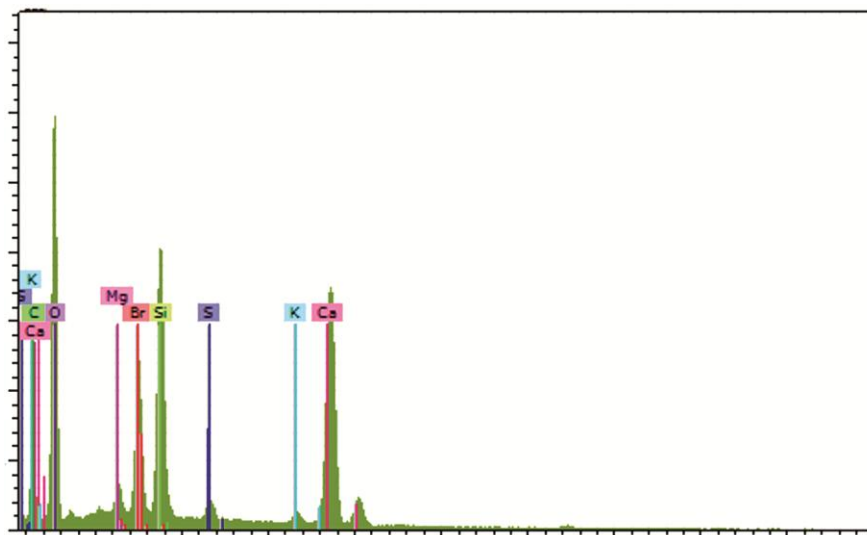


Fig. 3 — Elemental composition of PP fibres.

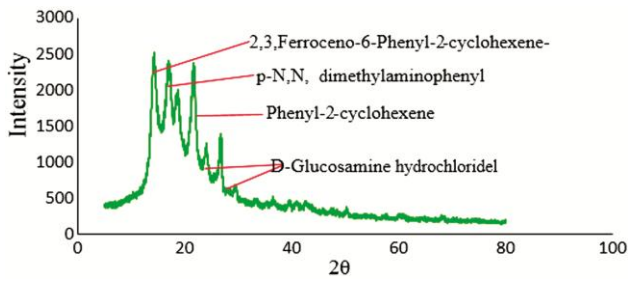


Fig. 4 — XRD pattern of PP fibers.

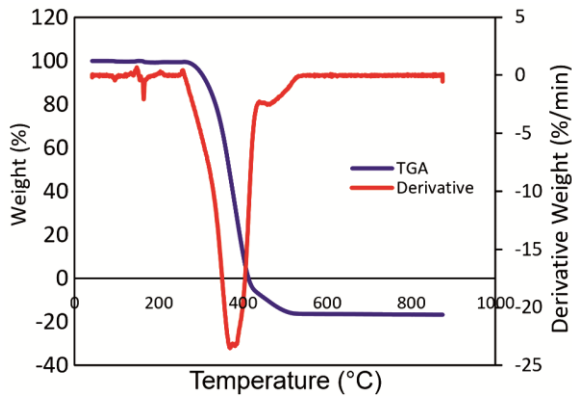


Fig. 5 — TG-DTA curve for PP fibers.

PP fibres, which illustrates how the fibre behaves under heat circumstances. According to the TGA and DTA curve in Fig. 5, PP fibres melt at temperatures between 170°C and 200 °C and become vapour by 341 °C. It is visible that they show a very small dilatation at melting at 15%.

### 2.3 Mix design

In this investigation, a mix with a W/C ratio of 0.4 was prepared with polypropylene fibres at 0.25% volume fraction. The compressive strength of the trial concrete mix after 7 days was checked and the appropriate mix has been finalized based on the fact that the strength at 7 days should have a minimum of 60% of the target strength. The finalized trial mix is then checked for the fiber-reinforced concrete also.

### 2.4 Mixing and casting details of specimens

Before mixing each batch, the mixer was thoroughly washed and cleaned before each batching to ensure that it was free of any other chemicals or impurities. While mixing, coarse and fine aggregates were added in equal parts and mixed for one minute. A small amount of water is added to the mix to ensure that the cement and fibres adhere to the aggregate. The mix was now supplemented with complete aggregates and cement. It is rotated for another half-minute. As shown in Fig. 6, the remaining fibres are then added back into the mix. 60% water is now



Fig. 6 — Final view of polypropylene fibres concrete mix.

added to the mixture. The superplasticizer is then thoroughly mixed with the remaining water and thoroughly stirred. After that, it is poured into the mix. Because superplasticizers act as lubricants, we needed to run the mix for 4-5 minutes to achieve a well-homogeneous mix at the end. In this study, PP fibre-reinforced concrete specimens were cast alongside control specimens. To examine the effect of fibre in concrete, the fibre dosage was varied. To determine the optimal percentage of fibres in concrete and compare the results with control specimens, fibres were added in the same proportion of the mix with different volumes of PP fibers. Various test specimens were created. Polypropylene fibres were added to the concrete mix at 0.25%, 0.75%, 1%, and 1.25% by volume fraction. The specimen moulds were checked and fixed as per the specifications specified in IS 10086: 1982<sup>35</sup>. For compressive strength testing, cubes of standard size 150 × 150 × 150 mm and cylinders of 150 mm diameter x 300 mm height conforming to IS: 10086: (1982)<sup>35</sup> were cast. Split tensile strength was tested using cylinders measuring 150 × 300. To evaluate the residual behaviour of the concrete specimens after exposure to higher temperatures, cubes of size 100 × 100 × 100 mm and cylinders of size 100 mm diameter × 200 mm were also cast.

### 2.5 Experimental investigations

In this investigation, concrete samples are heated in a muffle furnace to temperatures ranging from 200 to 1000 °C. Four thermocouples incorporated inside the furnace allow for exact temperature monitoring. K-type thermocouples that are attached to the surface of the specimens and connected to a digital data logger,

which is taken into account for the temperature exposure in the study, are used to measure the surface temperature of the samples. The furnace's temperature rises on average at a pace of  $10^{\circ}\text{C}/\text{minute}$ . The specimens are kept inside the furnace with an exposure to desired temperature followed by a cooling phase in which the specimens are allowed to cool within the furnace at ambient temperature as shown in Fig. 7. Figure 8 depicts a typical temperature exposure of the specimens at  $1000^{\circ}\text{C}$ . This is an imitation of ISO 834<sup>36</sup> Fire curve. During the heating phase, the specimen's surface temperature is set at  $1000^{\circ}\text{C}$ , and a continuous heating rate is used. After 600 minutes, it was noticed that the surface had reached the desired temperature of  $1000^{\circ}\text{C}$ . The surface temperature is then maintained for two hours during the exposure phase by keeping the temperature between  $1000 \pm 10^{\circ}\text{C}$ . The specimens are allowed to gradually reduce to room temperature inside the furnace during the cooling phase.

The samples are carefully taken out of the furnace after two hours, their weights are noted, and they are then put back inside to cool to room temperature. To determine the extent of damage in concrete specimens, samples are ultimately removed after 12 hours and visual observations are made about colour changes, weight loss, cracking patterns, and crack widths. A non-destructive test using ultrasonic pulse velocity (UPV) is also carried out. The visual investigation, non-destructive testing and mechanical

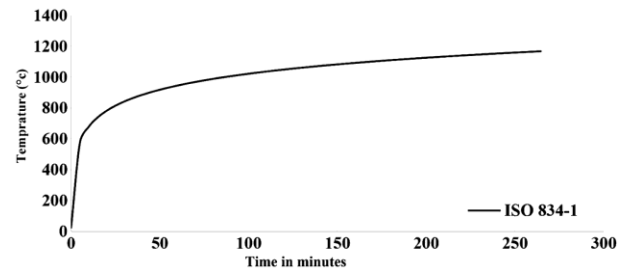


Fig. 8 — Temperature versus time graph in a muffle furnace.



Fig. 7 — Experimental setup for furnace.

properties such as compressive strength and elastic modulus of control specimens and temperature-exposed specimens are compared.

### 3 Results and Discussion

#### 3.1 Visual investigation

Concrete specimens were exposed to a range of temperatures, allowed to cool, and then underwent visual evaluation. Inspection revealed the change in surface and colour, which was noted. The images of polypropylene fibre reinforced concrete (PFRC) with volume of PP fibres were also taken to ascertain the colour changes as shown in Fig. 9. The change in colour on the concrete surface with respect to temperature increase was also noted. With the increase in temperature, the colour of concrete changes from dark grey to buff colour. The colour of the concrete turns pink colour around 400-600°C which indicates the presence of iron compound in the fine or coarse aggregate.

At 1000°C, the whitish-grey or white colour of the concrete was probably due to the dissociation of calcium carbonate or lime that is present in cement. The damages to the concrete after being subjected to elevated temperature can be approximately detected by observing the surface of the concrete. There was

no visible change in the texture of the concrete surface up to 400°C for PFRC, but slight cracks were observed in the control specimens which is subjected was 400°C as shown below. Beyond 400°C concrete started to crack when the temperature reached 600°C and control specimens showed pronounced cracks at 1000°C.

In this visual inspection, the cracks that developed as a result of the concrete being exposed were observed, and the diameter of each fracture was measured using a crack-width microscope, as shown in Fig. 10.



Fig. 10 — Crack-width measuring microscope.

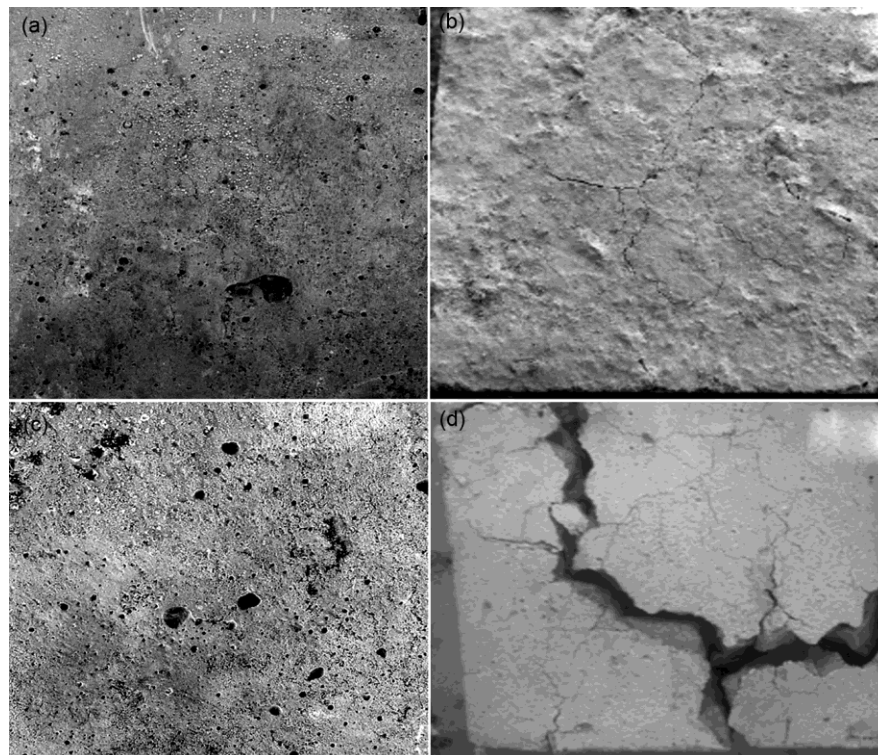


Fig. 9 — Surface damages of PFRC ( $V_f = 0.5\%$ ) after temperature exposure.

Table 3 — Crack width measurement of control and PFRC mixes with exposed temperature.

Type	The average width of the crack (mm)				
	200°C	400°C	600°C	800°C	1000°C
Control	No cracks	0.02 - 0.03	0.24 - 0.3	0.34 - 0.4	0.5 - 1.0
PFRC	No cracks	No cracks	0.026 - 0.032	0.18 - 0.2	0.2 - 0.4

Through a small crack-width microscope, the defects in concrete that result in cracks on the surface of the concrete when subjected to temperature were observed. Additionally, the crack's width is gauged. The damages in concrete in terms of cracks on the surface of concrete when exposed to temperature, were seen through a small crack-width microscope. The width of the crack is also measured. The measured crack widths are reported in Table 3 and presented in Fig. 11.

From Table 3, it can be observed that there were no visible cracks appeared till 400°C for PFRC whereas in the control specimen, there was a slight appearance of crack of width 0.02-0.03 mm.

Regarding the choice of PP fiber diameter, a common misunderstanding arises when comparing fibers at the same dosage. This approach actually involves comparing different total numbers of fibers, which ultimately highlights the benefits of thinner fibers. In our experimental study, alongside 17-micron fibers, we also included 30-micron fibers to examine the effect of diameter on cracks with an equal number of fibers. It was observed that in PP fiber reinforced mortar, the expansion of PP fibers during their phase change can induce damage, leading to cracking at the fiber-mortar interface. This damage and cracking tend to increase with the diameter of PP fibers. However, these cracks are typically small and remain disconnected from one another, resulting in an increase in local permeability of heated concrete without significantly affecting its overall permeability and, consequently, the spalling mechanism. Therefore, transitioning from 17 to 30µm diameter fibers would have a negligible impact on the effectiveness of PP fibers in preventing spalling.

For PFRC, cracks increased gradually and reached a maximum width of 0.2 mm when temperature increased at 800°C, whereas for control specimens it increased about 0.34 mm of crack width. This demonstrates that by addition of the fibres in concrete arrest the cracks and so stop the fissures from spreading further. However, in control specimens, fissures grow and spread.

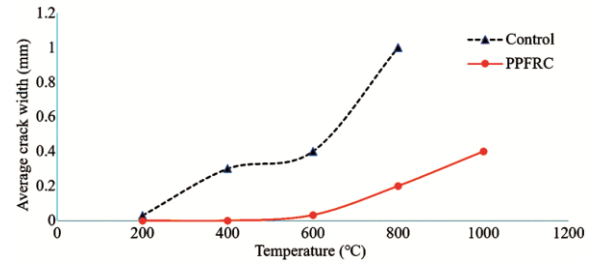


Fig. 11 — Crack width measurement of control and PFRC mixes with exposed temperature.



Fig. 12 — Digital balance for measuring mass.

### 3.2 Residual mass loss

In general, when exposed to higher temperatures, concrete mass decreases. This is caused by a variety of physico-chemical modifications like material evaporation, decomposition, and sublimation in concrete. Concrete is a heterogeneous material, therefore the many constituents in it cause physico-chemical changes that occur at varying temperatures. Density and mass are directly proportional. Thus, along with the loss of mass, density also decreases. In this experiment, a digital balance was used to record the mass loss for each group of specimens, as shown in Fig. 12. The specimens' weight was initially determined before exposure and immediately following an hour of cooling. The difference in mass obtained after exposure is known as residual mass, and it was noted. This test aids in predicting the

degree of decay in the structure when exposed to fire. The mass of the specimens was measured after one hour and 12 hours of cooling to determine the increase in mass of the specimens. It can be seen from Figs 13 and 14, that there was no significant weight loss up to 200°C. Beyond that, the mass gradually decreases. This was most likely due to the cement paste losing its binding property due to water evaporation in the C-S-H structure. The mass loss of the control specimen at 1000°C was approximately 12%, but it was nearly 6% in PFRC.

When compared to PFRC, mass loss in control specimens was nearly twice as great. This was because fibres prevented water in C-S-H from evaporating, thereby combining all of the materials and making the concrete denser. Furthermore, after 12 hours of cooling, there was a slight increase in mass, which could be attributed to moisture absorption from the atmosphere by the specimens.

**3.3 Ultrasonic pulse velocity test**

A non-destructive testing technique called ultrasonic pulse velocity (UPV) is used to evaluate the integrity and homogeneity of concrete without causing harm to it. The time it takes an ultrasonic pulse to travel a known distance in the concrete being tested is measured ( $V=L/T$ ). An impulse machine generates three types of waves, one of which was used in this study: longitudinal waves, also known as compressional waves. In this study, the instrument was used for UPV analysis of fire-exposed concrete, as shown in Fig. 15. Before beginning the experiment, the surface of the concrete was thoroughly rubbed with sandpaper, and petroleum jelly or grease was applied to the surface to connect the transducer. The probe amplitude and gain were set to 120V and 5x,

respectively, and the wave velocity of control and PPFR specimens, after exposure to different temperatures was measured as shown in Figs 16 and 17. For each specimen, the recorded velocity of the

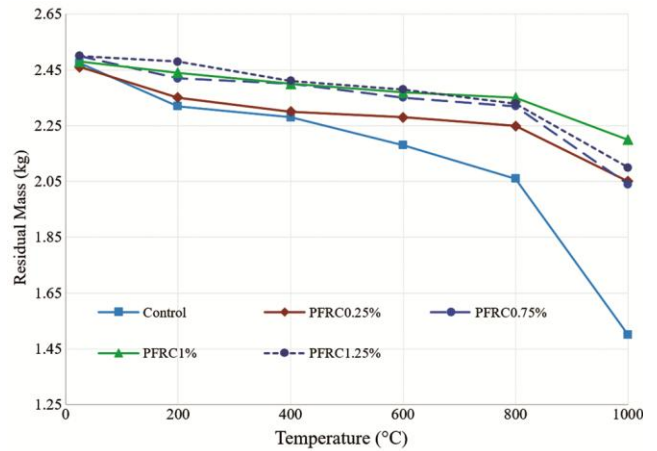


Fig. 14 — Mass loss of different concrete mixes after 1 hour cooling.



Fig. 15 — UPV test setup.

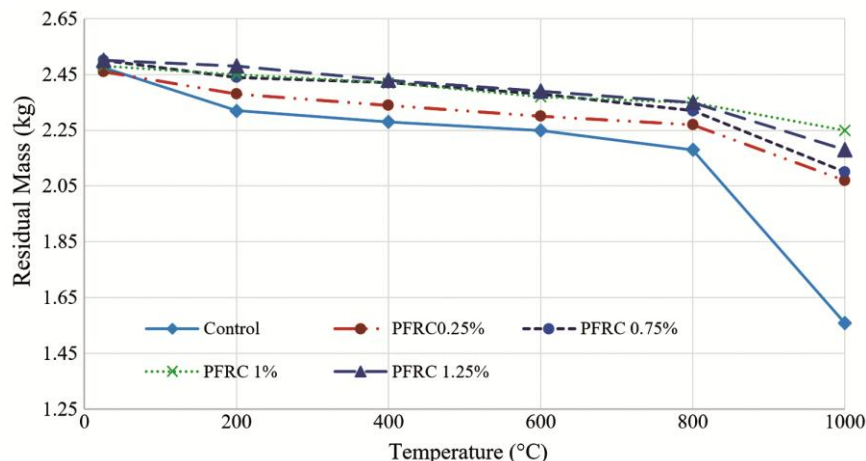


Fig. 13 — Mass loss of different concrete mixes after 12-hour cooling.

concrete was plotted against the temperature exposed. Using this NDT method, a qualitative idea for the concrete reinforced with fibres after exposure to elevated temperature was obtained. Wave propagation was also investigated.

Before and following exposure to various temperatures, the ultrasonic pulse velocity was measured and the results are shown in Table 4. As the temperature rises, the quality of the concrete deteriorates gradually. The pulse velocity of PFRC was initially higher at ambient temperature, indicating that concrete was denser and more compact in nature. PFRC outperformed control concrete in terms of quality.

The velocity of concrete decreases as it is exposed to higher temperatures. It was because the density of

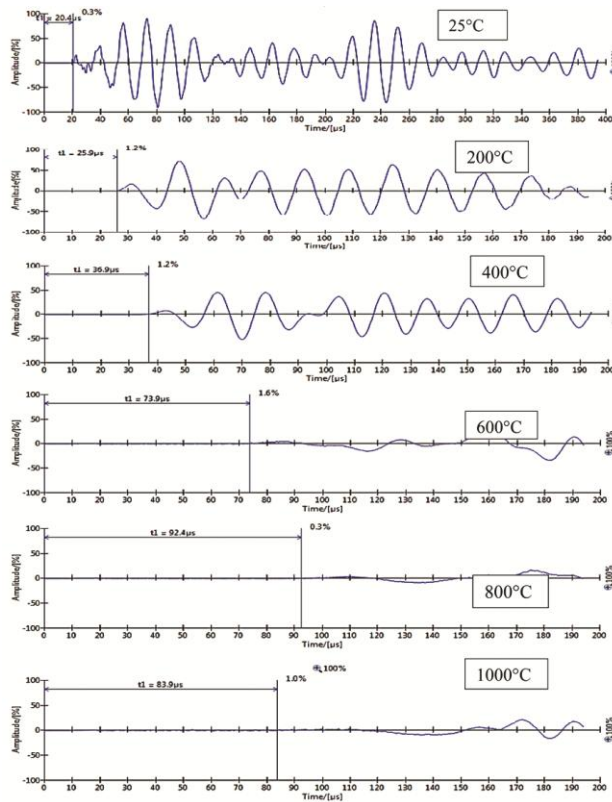


Fig. 16 — UPV wave pattern for control specimens.

concrete decreases, and there may be some internal and surficial cracks, etc., which can cause the wave to travel more slowly. The average velocity obtained was plotted against temperature and it is shown in Fig. 18. The temperature was found to decrease the amplitude of the wave while increasing the probe gain. The probe gain is a measurement of the intensity

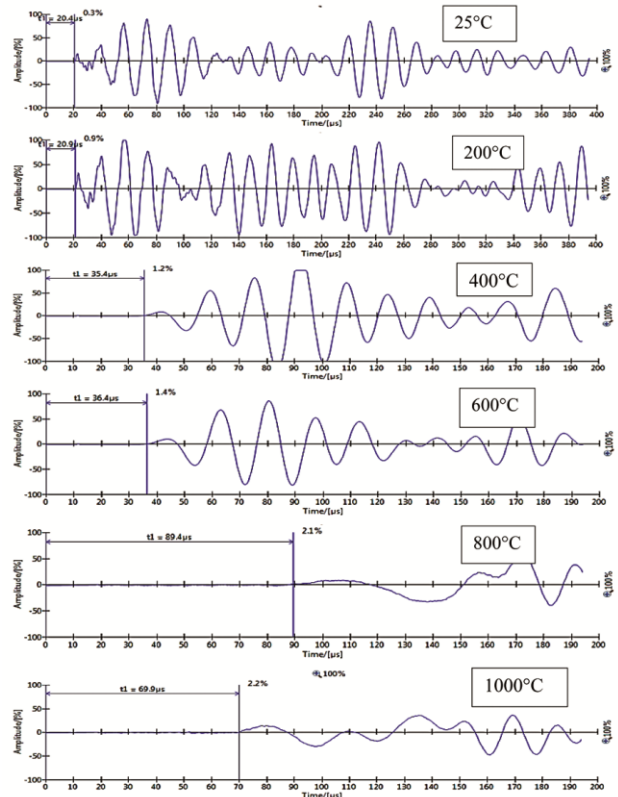


Fig. 17 — UPV wave pattern for PFRC.

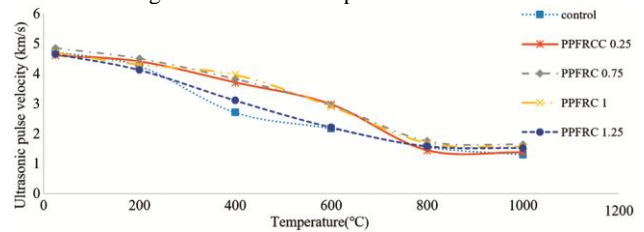


Fig. 18 — Ultrasonic pulse velocity (UPV) for PFRC.

Table 4 — Average pulse velocity at different temperatures.

Temperature (°C)	Mix designation				
	Control	PFRC0.25	PFRC0.75	PFRC 1	PFRC 1.25
25	4.72	4.6	4.85	4.7	4.65
200	4.25	4.4	4.5	4.3	4.12
400	2.7	3.7	3.82	3.96	3.1
600	2.17	2.97	2.96	2.9	2.2
800	1.55	1.44	1.75	1.68	1.57
1000	1.3	1.37	1.64	1.56	1.51

of the UPV wave passing through the specimens. As the temperature rises, the probe gain must be increased to obtain a proper wave pattern. This demonstrated that there is a flaw in the concrete. Furthermore, wave attenuation decreases with increasing concrete exposure temperature because density decreases. There was some distortion in the PFRC specimen that was exposed to 200°C. This demonstrates that the PP fibres have melted and a passage has formed, and because waves require a solid phase to travel, they may be unable to travel through the passage formed by the PP fibres. At 1000°C, the wave pattern for all specimens was almost nil or the amplitude was reduced, which could be attributed to the formation of multiple cracks and the creation of voids within the concrete.

**3.4 Residual compressive strength**

As concrete is exposed to temperature, properties of the concrete begin to deteriorate subsequently. Properties especially strength, elastic modulus, density etc. reduces as temperature increases. The compressive strength of the concrete is very important as it measures the capacity of the concrete to withstand load without any crack or failure. Hence, it is necessary to measure the strength of the concrete after exposure to the temperature.

Residual compressive strength was studied after the cooling regime and evaluate the residual strength in concrete after exposure to temperature. It is necessary to investigate the percentage loss or to evaluate how much strength that is remaining in concrete and to compare them concerning each set of temperatures of specimens. A universal testing machine of capacity 1000 KN was used to evaluate the residual strength as shown in Fig. 19. This test also helps us to understand the failure pattern of the concrete after exposure to higher temperatures. The study about the spalling effect, a sudden drop in stress etc. can be noted through this test. The test was generally done after a cooling period of 24 hours. The obtained strength is then tabulated against the temperature

and the trend of the residual strength is shown in Table 5.

Figure 20 shows that with increasing in temperature up to 200°C, the strength of concrete increases and thus decreases. When compared to control specimens, PFRC exhibits less strength loss. For example, the strength of the control specimen decreased by nearly 45-50% from ambient to 800°C, whereas the PFRC specimen decreased by only 32%.

A correlation of compressive strength with exposure temperature at different PP fibre content was carried out. Equation 1 to 5, show the relation between the compressive strength of control and PFRC specimens with the exposed temperature.

$$f_{c0} = -2E - 05t^2 - 0.0102t + 37.157 \quad \dots (1)$$



Fig. 19 — UTM for compressive strength.

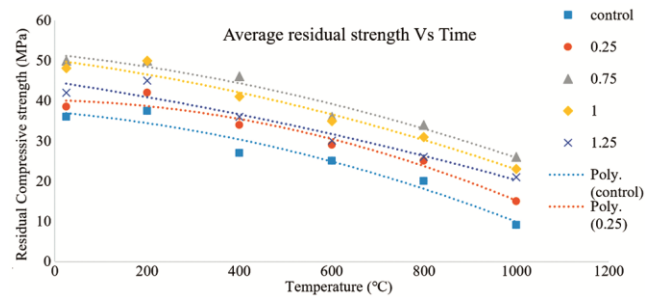


Fig. 20 — Ultrasonic pulse velocity for PFRC.

Table 5 — Average residual compressive strength.

Temperature (°C)	Average compressive strength (MPa)				
	Control	PFRC 0.25	PFRC 0.75	PFRC 1	PFRC 1.25
25	36	38.5	50	48	42
200	37	42	50	50	45
400	27	34	46	41	36
600	25	29	36	35	30
800	20	25	34	31	26
1000	9	15	26	23	21

$$f_{c_{0.25}} = -2E - 05t^2 - 0.0027t + 40.086 \quad \dots (2)$$

$$f_{c_{0.75}} = -1E - 05t^2 - 0.0126t + 51.493 \quad \dots (3)$$

$$f_{c_1} = -1E - 05t^2 - 0.0154t + 50.087 \quad \dots (4)$$

$$f_{c_{1.25}} = -7E - 06t^2 - 0.0174t + 44.664 \quad \dots (5)$$

Where,

$f_c$  = Compressive strength at a particular exposure temperature;

$t$  = Exposure temperature

The above equations can be used to predict the compressive strength at different PP fibre content at any temperature exposure. The PP fibre dosage varies between 0.25% and 1.25%. Similarly, the relation between compressive strength and UPV value of control and PFRC was proposed as given below in Eqs. 6 to 10. Fig. 21 shows a correlation between Compressive strength and UPV with varying percentages of PP fibres. The measured UPV was used to predict its compressive strength at different PP fibre content ranging from 0.25% to 1.25%. The figure shows the UPV values ranging between 1.5 to 4.85. UPV values above 4.5 indicate the excellent quality of concrete. Linear regression values recorded a good agreement correlation between UPV and Compressive strength for which  $R^2$  values are above 0.9. UPV is directly proportional to compressive strength.

Control Specimens

$$y = -3E - 06x^2 + 0.0225x - 12.717 \quad \dots (6)$$

$V_f = 0.25\%$

$$y = -2E - 07x^2 + 0.0078x + 9.5719 \quad \dots (7)$$

$V_f = 0.75\%$

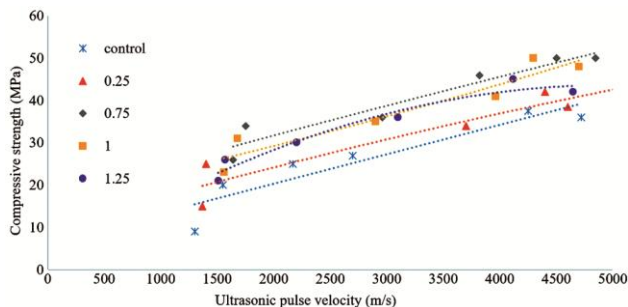


Fig. 21 — Relationship between UPV and compressive strength with PP fibre content.

$$y = -1E - 07x^2 + 0.0076x + 17.012 \quad \dots (8)$$

$V_f = 1\%$

$$y = 3E - 07x^2 + 0.0056x + 16.929 \quad \dots (9)$$

$V_f = 1.25\%$

$$y = -2E - 06x^2 + 0.017x + 1.0165 \quad \dots (10)$$

Where,

$x$  = ultrasonic pulse velocity (in m/s)

$y$  = Compressive strength (in MPa)

**3.5 Split tensile strength**

An indirect method of assessing the tensile strength capability of concrete is the split-tensile strength test. During the test, a diametric, compressive force is applied along the length of the cylindrical specimen. Concrete is well known to be weak in tension; to eliminate this problem, the use of fibres became critical. The concrete cylinder was loaded in compression on its side along a diameter plane in a Universal testing machine, as shown in Fig. 22 and the split tensile strength of the concrete was measured. The cylinder splitting along the loaded plane is the most common cause of failure.

From the theory of tensile strength concepts, the following formula is used for the evaluation of the splitting tensile strength,  $f_{ct}$  is given by;

$$f_{ct} = \frac{2P}{\pi dl} \quad \dots (11)$$

Where,

$f_{ct}$  - Split Tensile strength (MPa)

P - Ultimate Load (N)

D - Diameter of the cylinder (mm)

L - Length of the cylinder (mm)

Split tensile strength results obtained are shown in Fig. 23. The PP fiber has a 48% (maximum) increase



Fig. 22 — Split tensile strength test on cylinders.

in split tensile strength with comparison to control specimens. This shows that the addition of fibers in concrete significantly increases split tensile strength in concrete. It was also observed that with the addition of PP fibers split tensile strength gained more in 28 days i.e. at the early stage as compared to later age strength.

**3.6 Flexural strength**

The flexural strength test was performed on the same Universal Testing Machine (UTM). Applying the failure load on a prismatic specimen with dimensions of 100 mm x 100 mm x 500 mm after 28 days of curing, using the universal testing machine with a 100-tonne capacity under four-point loading at a rate of 0.5 mm/min, allowed researchers to determine the concrete's flexural tensile strength or modulus of rupture. The testing machine can assess flexural strength by IS 516. The specimens were held on the roller support so that the prism loading arrangements were four-point loading.

The flexural strength of PFRC is shown in Fig. 24. The increase in flexural strength PFRC is 51% (maximum). This may be because PP fibres arrest micro cracks. Beyond 0.75% of fiber content, there is a slight decrease in flexural strength. This may be due to balling effect of fibers in concrete.

**3.7 Failure modes**

On application of load on the control specimen tested at ambient temperature showed a brittle failure.

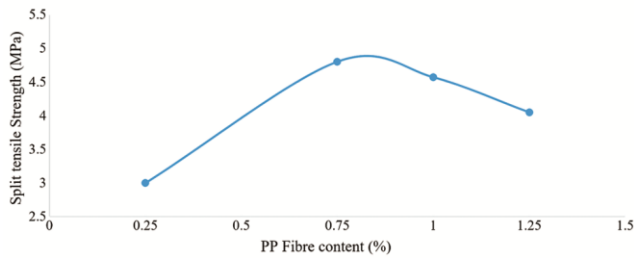


Fig. 23 — Spilt tensile strength with PP fiber content.

It fails with a loud explosive sound during testing. In the split tensile strength test it was observed that the cylinder under the maximum load failed exactly in the middle with fewer cracks as shown in Fig. 25. The four-point loading test on the prism revealed that vertical cracks at the bottom of the prism and in the centre or mid-span indicate the presence of a positive flexural crack in the prism's tension zone as shown in Fig. 26. During compressive strength test on PFRC, a simple small crack was only observed as shown in Fig. 27. Polypropylene fibers showed better tensile property when compared to the control specimen.

**3.8 Microstructural study**

Microstructural study of various concrete specimens at their respective exposure temperature was carried out using Scanning electron microscope (SEM) analysis. SEM images for each control and PFRC specimens at their respective temperature are shown in Fig. 28 and 29. SEM images of control specimens at various exposure temperatures are taken and shown in Fig. 28. It can be seen that at ambient temperature (25°C), C-S-H, ettringite (needle shape) were clearly seen. After 200°C exposure there is an increase in C-S-H and concrete became dense and compact in nature. This helps us to understand the reason for a slight increase in the strength of concrete after 200°C exposure. However, as temperature increases, the dissociation of C-S-H can be seen. The

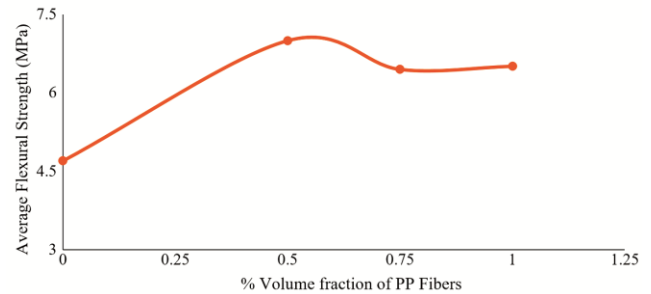


Fig. 24 — Flexural strength of PP fibres in concrete.



Fig. 25 — Failure of cylinders in split-tensile strength.



Fig. 26 — Failure of prisms in flexural testing.

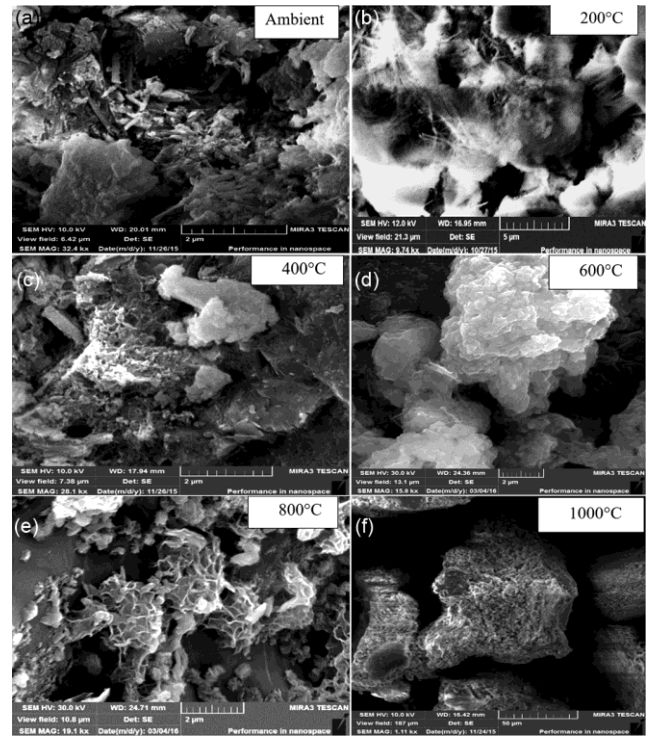


Fig. 28 — SEM images of control specimens.

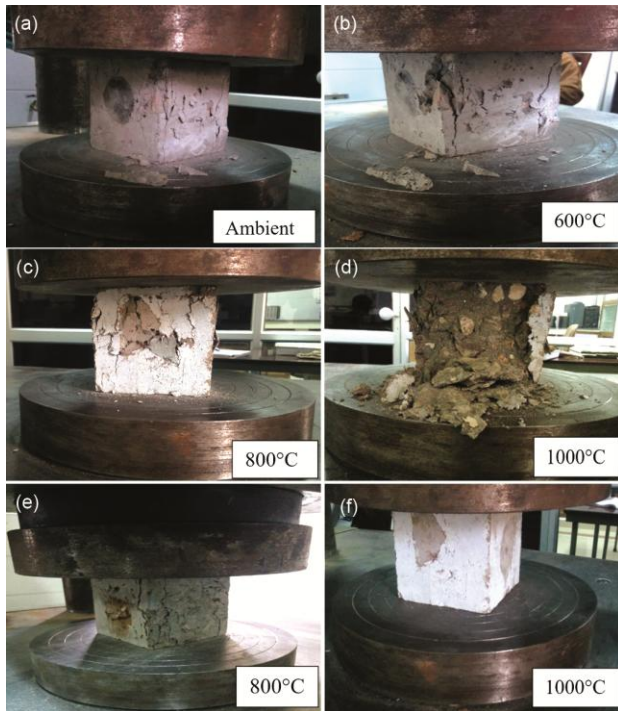


Fig. 27 — Failure of cubes in residual compressive testing.

dense structure was not seen and C-S-H crystals appeared to be stand separately and randomly distributed. The concrete exposed to 800°C appeared that almost all C-S-H was lost and cracks were also prominently visible.

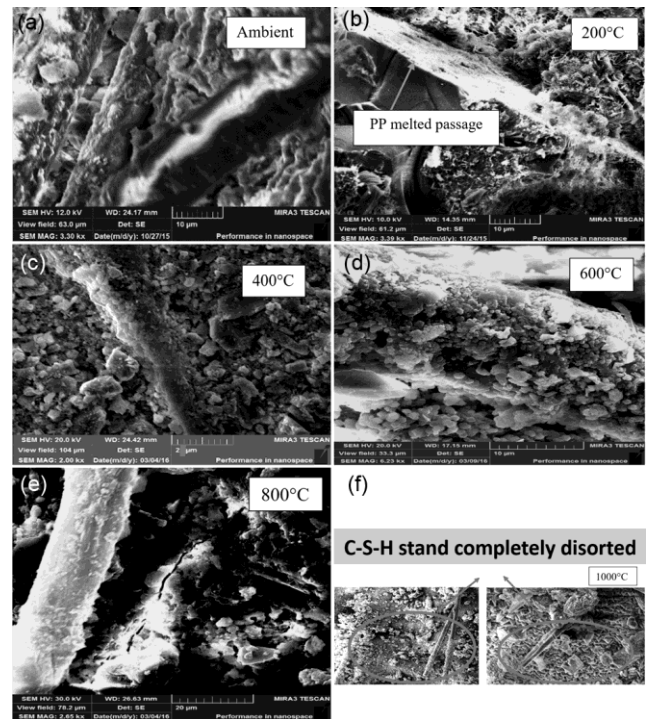


Fig. 29 — SEM images of PFRC specimens.

The presence of C-S-H on the fibres and a lot of ettringite nearby proves that there is bonding with cement particles, as shown in Fig. 29. Around 160–170°C, PP fibres begin to melt, creating a

passage that aids in relieving the concrete's excessive pore pressure. This PP fibre passage was clearly visible in the SEM image of PFRC at 200°C. The image of PFRC exposed to 800°C shows that fibres were attached to C-S-H and passages were formed due to PP fibres even at that temperature. It was also discovered that micro-cracks formed and that there were a lot of fibres surrounding the cracks. It was also discovered that micro-cracks formed, with a large number of fibres arresting them. This helps us to understand the mechanism of PP at these temperatures.

#### 4 Conclusion

Based on the experimental investigations carried out on different specimens at elevated temperatures and the results analyzed following conclusions are drawn below:

The cracks are observed gradually developing at elevated temperatures. With longer length fibers, the crack width is lesser as compared to the smaller length fibers and thereby helps in the arresting of the crack.

The results of this work have allowed a better understanding of the influence of fiber dosage and geometry on reducing fire spalling of normal strength concrete. The optimum dosage of PP fibers came out to be 0.75%. Any further increase in the dosage would lead to balling effect of the fibers. The dosage is lesser with the macro filament long length PP fibers of length 24mm.

When considering the choice of polypropylene (PP) fiber diameter, a common misconception arises when comparing fibers at the same dosage. This comparison actually entails different total numbers of fibers, ultimately demonstrating the advantage of thinner fibers. Comparing with the literature the literature no influence of fiber diameter on spalling is observed.

Ultrasonic pulse velocity of the concrete specimens decreases as the temperature increases. The decrease in pulse velocity is about 60% after exposure to 1000°C. In addition, the wave propagation pattern shows that there has been a decrease in amplitude and probe gain which was maybe due to the melting of PP fibers and the formation of passages.

The reduction in strength of control and PFRC specimens exposed to 1000 °C is in order of 75% and 42% respectively as compared to their strength at ambient temperature which is comparable with the small length fibers of higher dosage.

The increase in flexural strength of PFRC was about 51% when compared to control concrete which is same as the small length fibers with higher dosage.

The residual compressive strength decreases with an increase in temperature. The reduction is 52% of strength after 1000°C exposure.

Micrograph shows the changes occurring in concrete specimens during the time exposure. Passage created by PP fibers after their melting, formation of C-S-H on fibers, and formation of micro-cracks in control specimens were found. It can be concluded that PP fibers melt and create a passage that helps in the prevention of spalling. In addition, arresting of micro-cracks fibers was clearly visible which reveals no more propagation of thermal cracks.

#### Acknowledgment

The authors are grateful to the CSIR-CBRI for granting the permission to publish this work. The authors would also like to thank to officials of Fire Safety Engineering for allowing us to carry out experimental studies.

#### References

- 1 Kodur V, Properties of concrete at elevated temperatures, *International Scholarly Research Notices*, 2014.
- 2 Handoo S K, Agarwal S & Agarwal S K, *Cement Concrete Res*, 32(7) (2002) 1009.
- 3 Khoury G A, *Progress Struct Eng Mater*, 2.4 (2000) 429.
- 4 Kalifa P, Chene G & Galle C, *Cement Concrete Res*, 31(10) (2001)1487.
- 5 Bilodeau A, Kodur V K R & Hoff G C, *Cement Concrete Compos*, 26(2) (2004) 163.
- 6 Han C G, Hwang Y S, Yang S H & Gowripalan N, *Cement Concrete Res*, 35(9) (2005) 1747.
- 7 Shuttleworth P, Fire protection of precast concrete tunnel linings on the Channel Tunnel Rail Link, *Int GRCA Congress*, 35(4) (2001) 38.
- 8 Heo Y S, Sanjayan J G, Han C G & Han M C, *Mater Struct*, 45 (2012) 325.
- 9 Khoury G A, *Magazine Concrete Res*, 60(3) (2008) 189.
- 10 Bednarek W H, Pauksza D, Szostak M & Szymańska J, *J Polym Res*, 28 (2021)1.
- 11 Li Y, Tan K H & Yang E H, *Construc Build Mater*, 169 (2018) 629.
- 12 Noumowe A, *Cement Concrete Res*, 35(11) (2005) 2192.
- 13 Hager I & Mróz K, *Mater*, 12(23) (2019) 3869.
- 14 Shuttleworth, P., 2001. Fire protection of precast concrete tunnel linings on the Channel Tunnel Rail Link. *Concrete* (London), 35(4), pp.38-39.
- 15 Askarnejad S & Rahbar N, *J Nanomech Micromech*, 7(2) (2017) 04017002.
- 16 Zhang D, Dasari A & Tan K H, *Cement Concrete Res*, 113 (2018)169.
- 17 Garboczi E J, Snyder K A, Douglas J F & Thorpe M F, *Physical review E*, 52(1) (1995) 819.

- 18 Bentz D P, *Mater J*, 97(3) (2000) 351.
- 19 Mazzucco G, Majorana C E & Salomoni V A, *Comput Struc*, 154 (2015)17.
- 20 Suhaendi S L & Horiguchi T, *Cement Concrete Res*, 36(9) (2006)1672.
- 21 Haniche R, Debicki G, Bouamrane A & Zeltz E, Gas transfers and flow process through concrete maintained in temperature. *2nd International RILEM workshop on concrete spalling due to fire exposure*, October (2011) (pp. 95-102).
- 22 Lu F & Fontana M, 2016. Effects of Polypropylene Fibers on Preventing Concrete Spalling in Fire. *Structures in Fire*.
- 23 Heo Y S, Sanjayan J G, Han C G & Han M C, *Mater Struct*, 45 (2012) 325.
- 24 Heo Y S, Sanjayan J G, Han C G & Han M C, *Mater Struct*, 44 (2011) 599.
- 25 Li Y, Tan K H & Yang E H, *Cement Concrete Compos*, 96 (2019)174.
- 26 Jansson R, 2008. Material properties related to fire spalling of concrete.
- 27 Knack I, New PP-fibre with exceptional melting characteristics for improved fire protection in concrete building. *1st International Workshop on Concrete Spalling Due to Fire Exposure, Leipzig Germany*, September (2009) (pp. 238-247).
- 28 Huismann S, Weise F, Meng B & Schneider U, *Mater Struct*, 45(2012) 793.
- 29 Pistol K, Weise F, Meng B & Diederichs U, *Adv Mater Res*, 897 (2014) 284.
- 30 Felicetti R, Monte F L & Pimienta P, *Cement Concrete Res*, 94 (2017)13.
- 31 Standard B, 2004. Eurocode 2: Design of concrete structures— Part, 1(1), p.230.
- 32 Standard I, 1989. 8112-1989, 43 Grade Ordinary Portland cement-Specification (First Revision). Bureau of Indian Standards, New Delhi.
- 33 IS 4031: determination of compressive strength of hydraulic cement, Bureau of Indian Standard, New Delhi, 1988.
- 34 IS: 2386 (Part I) – 1963, Indian Standard, Method of Test for Aggregates for Concrete, (Part I); Particle Size and Shape (Eleventh Reprints); Bureau of Indian Standard, New Delhi, India. August-1997.
- 35 IS 10086 (1982): Specification for moulds for use in tests of cement and concrete
- 36 ISO. (1975). “Fire resistance tests-elements of building construction.” International Standard ISO 834, Geneva.